Multi-objective Trajectory Optimization to Improve Ergonomics in Human Motion

Waldez Gomes, Pauline Maurice, Eloïse Dalin, Jean-Baptiste Mouret, Serena Ivaldi

Multi-objective Trajectory Optimization to Improve Ergonomics in Human Motion

Waldez Gomes[1], Pauline Maurice[1], Eloïse Dalin[1], Jean-Baptiste Mouret[1], Serena Ivaldi[1]

***Abstract*—Work-related musculoskeletal disorders are a major health issue often caused by awkward postures. Identifying and recommending more ergonomic body postures requires optimizing the worker's motion with respect to ergonomics criteria based on the human kinematic/kinetic state. However, many ergonomics scores assess different risks at different places of the human body, and therefore, optimizing for only one score might lead to postures that are either inefficient or that transfer the risk to a different location. We verified, in two work activities, that optimizing for a single ergonomics score may lead to motions that degrade scores other than the optimized one. To address this problem, we propose a multi-objective optimization approach that can find better Pareto-optimal trade-off motions that simultaneously optimize multiple scores. Our simulation-based framework is also user-specific and can be used to recommend ergonomic postures to workers with different body morphologies. Additionally, it can be used to generate ergonomic reference trajectories for robot controllers in human-robot collaboration.**

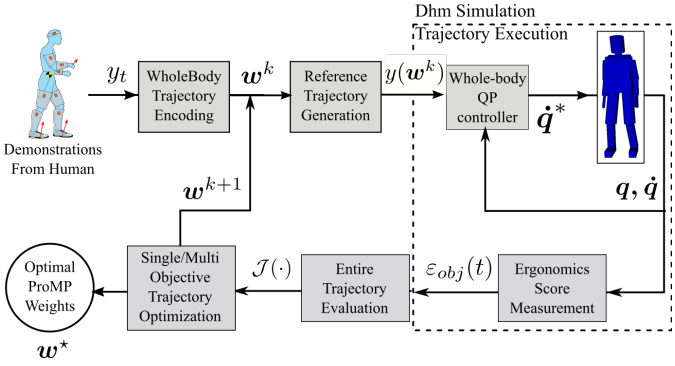

Fig. 1: Ergonomics human motion optimization framework. The entire motion is encoded into motion primitives that can be readily optimized with respect to a single, or multiple, ergonomics scores using a user-specific Digital Human Model (DHM) Simulation for motion evaluation.

I. INTRODUCTION

Work-related musculoskeletal disorders (WMSDs) are among the first causes of occupational diseases worldwide, representing a major health issue, with important costs for companies and society. They develop when biomechanical demands repeatedly exceed the workers' physical capacities, and, along with force exertion, awkward postures represent one of their major risk factors [1]. In many situations, workers are able to choose among a variety of postural strategies to execute a task. Yet, their natural choice does not always match the best strategy with respect to long-term health. For instance, several studies reported that novice workers can adopt strategies that result in higher biomechanical loading in comparison to experienced workers [2]. Recommending better ergonomic postures for specific tasks is, therefore, a promising avenue to help to reduce WMSDs among workers.

Posture recommendation requires a prior identification of the best postural strategy for each task –taking into account workplace constraints– adapted to the specific individual. The best strategy usually depends on individual factors, such as body morphology, or joint capacities. The question of identifying ergonomic postural strategies is also pushed forward by the growing interest in collaborative robotic assistance. In addition to the direct physical assistance they can provide, *e.g.*, through weight compensation, collaborative robots can be used to guide workers toward a more ergonomic posture via the positioning of their end-effector [3]–[6]. But such assistance also requires the knowledge of the user's optimal posture.

State-of-the-art human-robot applications that improve the human partner's ergonomics usually take in consideration only one ergonomics score [4]–[7]. However, single-objective optimization may not be sufficient to obtain "good" whole-body motions, since optimizing for only one criterion often produces motions that are less ergonomic in other body regions; e.g., minimizing only the back flexion ignores the leg motion or efforts at the shoulder joints.

To address this problem, in this paper we propose to use multi-objective optimization to generate several Pareto-optimal motions that simultaneously optimize several different ergonomics scores. We propose a simulation-based optimization framework to generate ergonomic whole-body motions for different body morphologies and activities (Fig. 1). Initial demonstrations from motion capture are used as feasible motions to warm-start the optimization process. The motions are parametrized by probabilistic movement primitives (ProMPs), that can encode several task demonstrations. A user-specific Digital Human Model (DHM) simulates the whole-body motion in a physics engine, and the simulation's output is used to estimate several ergonomics scores based not only on the body's posture, but also on its joint torques. A multi-objective optimization algorithm (NSGA-II) is used to generate several possible Pareto-optimal solutions (i.e.,

[1]The authors are with Université de Lorraine, CNRS, Inria, LORIA, F-54000 Nancy, France. waldez.azevedo-gomes-junior@inria.fr, surname.name(at)inria.fr

This work was supported by the European Union's Horizon 2020 Research and Innovation Programme under Grant Agreement No. 731540 (project AnDy).

whole-body motions) that represents trade-offs among the different ergonomics criteria. This approach is user and task specific, and generates a variety of different movements that promotes the different ergonomics criteria, producing more "ergonomically reasonable" motions of the DHM.

After describing the method in detail (section III), we empirically show that: 1) ergonomics optimization must be user-specific (experiment 1 in section IV-V); 2) optimizing for one single criteria may lead to non-ergonomic motions for other criteria, which means ergonomics criteria can conflict (experiment 2 in section IV-V); 3) optimizing simultaneously for several criteria using multi-objective optimization leads to a rich set of trade-offs motions that are more reasonable in terms of ergonomics and realistic for a DHM.

II. RELATED WORK

Prior work used human models to automate whole-body motion analysis for a given activity [8], [9]. There is a recent trend in the human-robot interaction community to use them to improve the human posture with respect to ergonomics scores during physical interactions. For instance, Marin *et al.* optimized a shared object's position in order to minimize the maximum muscle activation signal taken from a fast-to-compute musculoskeletal surrogate model [5]. Van der Spaa *et al.* optimized a discrete sequential plan of poses for a shared object during its transportation by both human and robot, with respect to the Rapid Entire Body Assessment (REBA) score, a standard whole-body ergonomics score [10].

Other work continuously evaluated the human kinematics/kinetics to try to influence the human posture with different robot actions. Shafti. *et al.* used wearable sensors to compute the Rapid Upper-Limb Assessment (RULA) score and adapt the robot's end-effector accordingly until the ergonomics evaluation is considered satisfactory [6]. Kim *et al.* minimized the human joint torque due to an external load [4]. Similar optimization techniques were used to improve human operator ergonomics during teleoperation [11], [12].

The examples above consider single ergonomics scores, however, given the multi-factorial causes of WMSDs, optimizing the movement for one ergonomics score could deteriorate other possible antagonistic scores. For this matter, there are some examples of multi-objective ergonomics optimization in the literature. For instance, Xiang *et al* optimized a human's posture w.r.t. ergonomics and stability scores [13], and Iriondo *et al* optimized a workstation setup parameter w.r.t RULA, and the human's upper-arm elevation angle [14]. In a physical human-robot application, Maurice *et al* optimized a robot's design parameters to simultaneously improve several ergonomics scores [15]. Figueredo *et al* combined muscle activation predictions and the REBA score to calculate a comfortability index that can be used in a physical human-robot interaction to guide the human partner towards postures that minimize both types of scores [16].

Here, we propose a framework to optimize human- and activity-specific whole-body motions w.r.t. several ergonomics scores. We also show that the resulting optimal motions are sensitive to different body morphologies, and ergonomics scores.

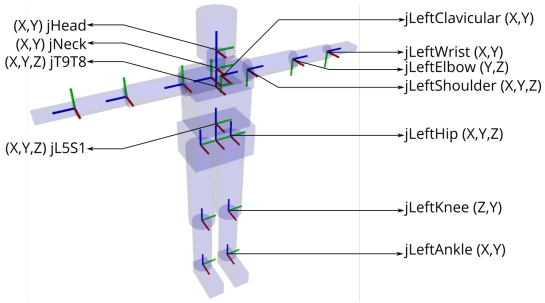

Fig. 2: Digital Human Model (DHM) joints description. The axes are X=Red, Y=Green, Z=Blue.

III. METHODS

A. Digital Human Model Simulation

The DHM used in this work (Fig. 2) consists of 19 rigid bodies linked together by 18 compound joints, for a total of 43 DoFs (11 for the back and neck, 9 for each arm including the sternoclavicular joint, and 7 for each leg), plus 6 DoFs for the free-floating base. Each DoF is a revolute joint controlled by a single actuator. Different human morphologies are easily generated from a desired body mass and height, by scaling the geometric and inertial parameters of the human model according to average anthropometric coefficients [17], [18].

The DHM is simulated in a physics engine (DART [19]) and controlled by a multi-task quadratic programming (QP) controller [20] that generates the motion that will be evaluated. The QP controller takes reference Cartesian trajectories of activity-defining body segments as input, and outputs desired joint velocities for the DHM. The QP is set to minimize the tracking error of these references while handling task priorities defined by the user. The priorities are defined by hierarchical levels, and tasks within the same level are further prioritized by their task weights. At the first priority level of the QP controller, there is a fixed Cartesian task for both feet that keeps the DHM in double support, and a task for the DHM's center of mass, to balance the DHM. At the second priority, there are Cartesian tasks for the hands, pelvis, and head, as well as a task that defines reference body postures. Here, the weights of all tasks are defined according to the work activity.

B. Ergonomics Evaluation

To obtain ergonomic motions from the optimization, we need to define ergonomics scores as objective functions to our formulation. There are many possible ergonomics scores typically representing different physiological phenomena that could increase the risk of developing WMSDs [21]. However, there is no strict consensus on a single score to use for motion optimization. Moreover, they might be antagonistic among themselves, *e.g.* the same movement could produce "good" results for a score, and "bad" results for another.

TABLE I: Ergonomic Evaluation Scores. $\varepsilon_{obj}(t)$ is the instantaneous score.

Description	Score	$\varepsilon_{\text{obj}}(t)$
RULA-C	Regression of RULA [22]	ε_{rc}
Normalized whole-body Effort	$\frac{1}{n_{joints}} \sum_{i \in joints} \left(\frac{\tau_t^i}{\tau_{max}^i} \right)^2$	ε_{nwe}
Torques Shoulder	$\|\boldsymbol{\tau}_{shoulder}\|$	ε_{tsh}
Torques Lumbar	$\|\boldsymbol{\tau}_{lumbar}\|$	ε_{tlb}
Back Flexion	$\left\|\theta^Y_{L5S1}\right\|$	$\varepsilon_{\text{back}}$

For this reason, instead of using an aggregated score, that is often task-specific, we consider several scores, ε_{obj}, separately (table I). In order to obtain an evaluation of the entire trajectory execution, we use a cost proportional to the squared RMS value of ε_{obj} for each score, for the entire activity duration:

$$\mathcal{J}_{obj} = \sum_{t \in [0 \dots T]} \varepsilon_{obj}^2(t) \tag{1}$$

where $T \in \mathbb{R}$ is the final simulation instant. Below, we describe each of the selected scores ε_{obj}.

RULA-C or RULA Continuous: The Rapid Upper Limb Assessment tool [22] is often used by ergonomists to evaluate work activities involving upper-body motion. It consists of a score ranging from 1 to 7, calculated based on the joint positions (posture), the force/load applied at the worker's arm, and how many times the activity is repeated. RULA time evolution during a work activity is likely to have discontinuities, and plateaus that make its domain exploration less efficient for many optimizers. To alleviate this problem, we propose a continuous version of RULA instead: RULA-C, $\varepsilon_{rc} \in \mathbb{R}^+$. To compute RULA-C, we fit second-degree polynomial functions to calculate intermediate scores for the RULA joints. The joint scores for each limb are combined with weighted sums whose weights are computed from linear regressions of the standard RULA tables. Moreover, differently from RULA, RULA-C only takes into account the body posture.

Normalized whole-body Effort: The torques at every joint are summed to quantify the whole-body effort (table I), where all joint torques are normalized w.r.t. average maximum human capacity [17] in order to handle the joint torque capabilities.

Local measurements: WMSDs at the shoulder and lumbar areas are among the most common in the population [1], therefore, we chose scores that target them. For the shoulder joint, we monitor its absolute torque values, ε_{tsh}, and for the lumbar joint, we monitor not its absolute torque values, ε_{tlb}, and the back flexion angle, ε_{back}.

C. Whole-body Trajectory Parameterization

The reference trajectories to the QP controller define the whole-body movement, from which, a few of them are selected to be optimized, and for this reason, parameterized by Probabilistic Movement Primitives (ProMPs), which can represent a set of movement demonstrations as Gaussian distributions [23]. The mean of those distributions are represented as a weighted sum of basis functions, $\boldsymbol{\phi}_t$, defined at the learning of the ProMP. Therefore, a ProMP mean trajectory, y_t^{traj}, can be modulated by its weight vector, $\boldsymbol{w}_{traj}$:

$$y_t^{traj} = \boldsymbol{\phi}_t^\top \boldsymbol{w}_{traj} \tag{2}$$

Similarly to [24], all ProMP trajectories can be stacked into a single weight vector, that finally defines our parameters to be optimized: $\boldsymbol{w} = [\boldsymbol{w}_1 \dots \boldsymbol{w}_{n_{trajs}}]$.

The initial ProMP trajectories are a result of estimating the weights, $\boldsymbol{w}$, according to the initial movement demonstrations captured using a whole-body motion capture system.

D. Trajectory Optimization

We optimize a selection of the DHM body segment trajectories, $\boldsymbol{y}(\boldsymbol{w})$, through its optimizable parameters, $\boldsymbol{w}$, w.r.t. one of the ergonomic scores in table I with a single-objective optimizer, or with several scores, simultaneously, with a multi-objective optimizer. Given an episode k in the optimization loop (Fig. 1), the point $\boldsymbol{w}^k$ is considered feasible if, and only if, the executions of the whole-body trajectories $\boldsymbol{y}(\boldsymbol{w}^k)$ respect some nonlinear constraints.

Trajectory Constraints: The DHM limbs and reference trajectories should always be within the environment workspace. That is, each ProMP weight is constrained to box boundaries that correspond to the DHM's reach in the workspace. Additionally, during the trajectories' execution, the DHM must never fall, and its hand(s) must reach all (activity-dependent) points of interest that are relevant for the activity. In order for the trajectory execution scores (1) to be comparable, the duration of every trajectory execution is always fixed for every episode. This trajectory optimization is, therefore, a derivative-free problem with black-box non-linear constraints.

Single-Objective Trajectory Optimization (SOTO): We bootstrap the optimization with the initial ProMP weights learned from the demonstration set. To optimize each one of the scores separately, we use single-objective optimization with the optimizer COBYLA (Constrained Optimization BY Linear Approximation) [25], a deterministic local optimizer that directly takes black-box constraints as inputs alongside any of the ergonomics scores accumulated by (1), and has already been used for constrained motion optimization problems [24]. The COBYLA implementation is taken from NLopt [26].

Multi-Objective Trajectory Optimization (MOTO): To optimize for multiple scores at the same time, we advocate for multi-objective optimization. The goal becomes not to find one single optimal solution, but rather, a *set* of Pareto-optimal solutions that provide trade-off trajectories for conflicting ergonomics scores, *i.e* a Pareto front. By definition [27], within the Pareto front, all solutions are said to be dominant: given solutions $\boldsymbol{w}_1$ and $\boldsymbol{w}_2$, $\boldsymbol{w}_1$ is said to dominate $\boldsymbol{w}_2$ if and only if $\boldsymbol{w}_1$ provides better results for all objective functions; if one or more of $\boldsymbol{w}_2$'s objectives is better than in $\boldsymbol{w}_1$, then, both are dominant solutions with a trade-off between each other. We used the Non-dominated Sorting Genetic Algorithm II (NSGA II), a multi-objective evolutionary optimizer [27] implemented in the C++ library Sferes$_{v2}$ [28].

Objective Function Penalties: Differently from COBYLA, NSGA-II's implementation does not handle specifying feasible/unfeasible points directly, so we modify the objective function (1) to penalize the unfeasible points. Each ergonomics score is penalized in case the DHM falls or it does not reach the activity's points of interest:

$$\mathcal{J}_{obj} = T_{fall}\mathcal{P}_{obj}^{fall} + \mathcal{P}_{obj}^{via} + \sum_{t\in[0\ldots T]} \varepsilon_{obj}^{2}(t) \tag{3}$$

where $T_{fall} \in \mathbb{R}^{+}$ is the period of time in which the DHM has been fallen, $\mathcal{P}_{obj}^{fall} \in \mathbb{R}^{+}$ is the fall penalty for a given score, and $\mathcal{P}_{obj}^{via} \in \mathbb{R}^{+}$ is the point-of-interest penalty for a given score. Each score is associated with a different penalty value for they have different orders of magnitude.

Bootstrapping Initial Demonstrations: NSGA-II's does not allow defining initial trajectories directly. Hence, we modify the initial population sampling in order to bootstrap the initial human demonstrations. The i-th variable, w_i, of each initial individual is sampled using the initial ProMP i-th variable, $w_i^{initial}$ using a Gaussian distribution:

$$w_i = \mathcal{N}(w_i^{initial}, \delta_i\beta) \tag{4}$$

where δ_i is the largest distance between $w_i^{initial}$ and any of its box boundaries, and $\beta \in \mathbb{R}$ is a constant that modulates how much of the boundaries we want to sample initially. For instance, if $\beta = \frac{1}{3}$, then $p(w_i = \text{boundary}_i) \leq 0.3\%$, that is, we would sample the entire workspace with very low probabilities at each variable boundary. Here, we chose $\beta = \frac{1}{12}$, a low value, to keep the initial sample close to the initial demonstrations.

IV. Experiments

The proposed framework is used to optimize whole-body motions under a variety of body morphologies, ergonomics scores, and work activities. Two work activities commonly related to movements that are risky in terms of ergonomics were analyzed, A and B (Fig. 3), which are described hereafter.

Activity A - Pick and Place Object from a Shelf: In this activity, a human has to reach an object located on a shelf with its right hand, take the object, and move it laterally toward the right side to another point on the same shelf. If the worker's shoulder level is below the shelf, this activity requires overhead work that could overload the worker's right shoulder.

To execute this activity, the DHM QP controller includes an additional task that commands the head to always face the right hand position. The task weights in the QP controller are set as: 1.0 for the feet position (X,Y,Z), CoM position (X,Y), and hand position(X,Y,Z); 0.5 for the hand orientation (roll, pitch, yaw); 0.1 for Pelvis position (Z), and Head orientation; 0.05 for a reference body posture task; and 0.005 for a reference back lateral bending joint position task.

Activity B - Lift Box from the Floor: In this activity, a human has to reach a box situated on the ground, in front of her/him, and with both hands, lift it to the waist level height. This activity commonly requires a great amount of effort surrounding the human's lumbar back area, which could be overloaded in the case of excessive back flexion, and/or excessive manipulated weights.

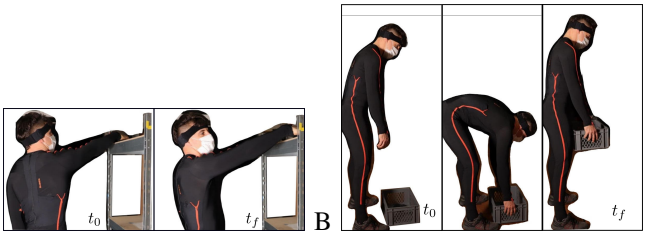

Fig. 3: Demonstrations for work activities A and B captured with the motion capture suit XSens MVN. A: Pick and place a weight on a high shelf. B: Lift a box from the floor.

To execute this activity, the weights in the QP controller are set as: 1.0 for the feet position (X,Y,Z), CoM position (X,Y), hand position and orientation (X,Y,Z, roll, pitch and yaw); 0.05 for the pelvis position and orientation (Z, pitch), and reference body posture task; and 0.05 for reference joint positions at the ankles, knees, and back internal rotation and abduction joint positions.

A. Experiment 1 - Effect of Varying Morphology

The goal of this experiment is to show that optimal ergonomic motions are user-dependent. We generated 9 different DHM morphologies with 3 different body heights, and 3 different body mass indexes corresponding to underweight, average weight, and overweight morphologies (Tab. II). In this experiment, the right hand vertical position and the center of mass (CoM) ground projection trajectories were optimized for an Activity A type of motion, in which the shelf is located at 1.5 m high and the start and end points for the hand are 30 cm apart. The initial hand trajectory was artificially generated as the minimum jerk trajectory between the start and end points. The hand trajectory was defined by a ProMP with 15 weights, and the CoM trajectory by a ProMP with 5 weights for each coordinate, X and Y, therefore, $\boldsymbol{w} \in \mathbb{R}^{25}$.

For each morphology, we ran single-objective optimizations with 2 relevant ergonomics scores for the shoulder: the RULA-C score (standard score to evaluate upper-body motions), and the shoulder torque score. The optimizer was set so that the optimization stopped after 1000 rollouts or when the improvement in cost function between successive rollouts was below 10^{-5}.

B. Experiment 2 - Effect of Ergonomics Scores

The goal of this experiment is to show that SOTO with different ergonomics scores generates different optimal trajectories with possible negative impact on the overall ergonomics due to conflicting criteria. We optimize the motion for both types of activities, A and B, and for each activity we run one SOTO for each ergonomics score listed in Table I. Differently from experiment 1, here, the initial motion is captured from real human demonstrations (Fig. 3). In activity A, the shelf is located at 1.7 m high, and the start and end points are 0.64

m apart. The human demonstrator, as well as his DHM, are 1.85 m high, with 93 kg, therefore, here, activity A required overshoulder work. For both activities, we instructed the human demonstrator to perfom a non-ergonomic demonstration (keeping hand above shoulder level in activity A and bending the back and not the knees in activity B), so that there was always a path for improvement in the optimization process. Additionally, weights of 1kg were used for both activities to limit the risk of injuries. In the simulation, however, we used a 5kg object (act. A) and a 10kg box (act. B) to assess demanding tasks where the choice of postural strategies might have a larger impact on ergonomics scores.

In activity A, the CoM, hand, and Pelvis QP reference trajectories are optimized with 10, 30, and 10 ProMP weights respectively, totaling 50 parameters to be optimized. In activity B, the CoM, and Pelvis QP reference trajectories are optimized with 10, 20 ProMP weights respectively, totaling 30 parameters to be optimized. For each parametrized trajectory, the initial values of the ProMP weights are learned from 5 human demonstrations. In both activities, the optimizer was set so that the optimization stopped after 1500 rollouts or when the improvement in cost function between successive rollouts was below 10^{-5}.

C. Experiment 3 - Multi-Objective Optimization

In this experiment, our goal is to show that MOTO generates motions with better trade-offs between several ergonomics scores than SOTO. We ran the MOTO on the same activities as in Exp.2, including the same constraints and parameters for the DHM QP controller. Instead of including all the ergonomics scores in the optimization, we selected the scores that are most relevant for each activity. Activity A demands a significant motion from the right shoulder, and it is predominantly an upper-body work activity, so we chose to optimize the motion w.r.t torques shoulder, normalized whole-body effort, and RULA-C scores. For activity B, both the shoulder and the lumbar joints are well demanded during the box lifting, so we chose to optimize the motion w.r.t. torques shoulder, and torques lumbar scores.

NSGA-II hyper-parameters are set as follows: cross rate = 0.5; population size $= 100$; number of generations $= 600$ (totalling 62000 rollouts per optimization execution). The mutation rates are set to 0.2, and 0.4 for activities A and B respectively, to take into account the different number of optimization parameters between activities. Since NSGA-II is a stochastic algorithm, we ran the optimization, in parallel, 20 times.

V. Results and Discussion

A. Experiment 1

The optimization generated motions with improved trajectory ergonomics scores for each one of the morphologies with a median improvement of 10.5% and IQR of 24.0% regarding the RULA-C score, as well as a median improvement of 41.1% and IQR of 35.0% for the torque shoulder score (table II). For the tall morphologies, m_1, m_2, m_3, and for both evaluated

TABLE II: Improvement of the ergonomics score from the initial movement after SOTO for different morphologies.

m_i	**Height (m)**	**B.M.I.**	**Weight (kg)**	$\mathcal{J}_{rc}$	$\mathcal{J}_{tsh}$
1	2.0	18	72	10.5%	27.1%
2	2.0	22	88	9.4%	42.3%
3	2.0	30	120	10.2%	30.2%
4	1.8	18	58	7.9%	37.8%
5	1.8	22	71	7.6%	24.1%
6	1.8	30	97	20.1%	74.8%
7	1.6	18	46	30.6%	58.2%
8	1.6	22	56	38.4%	41.1%
9	1.6	30	77	34.7%	69.1%

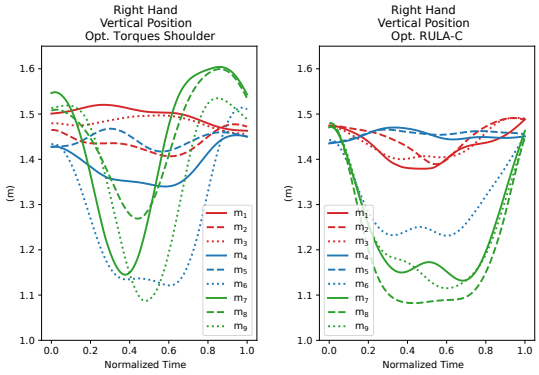

Fig. 4: Optimized hand trajectories w.r.t. torques shoulder and RULA-C scores for the 9 morphologies $m_i | i \in [1 \dots 9]$ in table II in exp. 1.

scores, the hand vertical trajectories did not vary much from the initial hand vertical trajectory in comparison with the short morphologies, m_7, m_8, m_9 (Fig. 4). This was likely because the initial hand vertical trajectory, set at 1.5 m high, was already well below the tall morphologies shoulder level, which is likely to characterize a local minima for both RULA-C and torque shoulder scores. The short morphologies, on the other hand, lowered their right hand as much as possible to avoid raising the arm to the shoulder level. **These results confirm that each individual needs to have a custom motion optimization for his/her body morphology.**

B. Experiment 2

Each optimization improved the initial motion according to its ergonomics score (Fig. 5). In Activity A, each optimization improved : back flexion by 99.37%, RULA-C by 4.52%, normalized whole-body efforts by 12.92%, torques shoulder by 60.36%, and torques lumbar by 77.24%. In Activity B, each optimization improved : back flexion by 93.42%, RULA-C by 30.02%, normalized whole-body efforts by 87.67%, torques shoulder by 64.97%, and torques lumbar by 67.32%.

Each one of the ergonomics scores have had a unique influence on the whole-body posture and efforts. For instance, the DHM's right elbow is more flexed during the optimal motion w.r.t. the torques shoulder score in comparison to the other motions during Activity A (Fig. 6). This is likely due

to the fact that flexing the elbow brings the arm closer to the torso, hence, decreasing the torques caused by gravity on the shoulder. During activity B, the initial motion has excessively high lumbar torques (Fig. 5) due to the large back flexion (Fig. 6). This motion strategy was penalized by all ergonomics scores, which in turn favored motions that reduce the back torque decreasing the DHM's back flexion, and increasing the DHM's knee flexion instead. Interestingly, this is the case even for the torque shoulder optimal motion, where the lumbar torque is not directly penalized, although with a lesser amount of knee flexion than the others.

The results confirm that solutions optimized for a given score may degrade other scores (Fig. 5). In activity A, minimizing the torque shoulder score increases the whole-body effort and back flexion, while in activity B, minimizing back flexion increases the torque shoulder score. Additionally, conflicting ergonomics scores could happen when optimizing for scores that do not evaluate the activity's main load requirements. For instance, in activity A, whose main load is at the shoulder, optimizing for back flexion highly increased torques at the shoulder, while optimizing for lumbar torques increased the whole-body efforts in comparison to the initial motion.

According to these results, optimizing for a single ergonomics score may not be advisable, and a more holistic approach concerning different ergonomics criteria must be sought for motion optimization.

C. Experiment 3

The Pareto front for both activities was computed for 20 MOTO replicates per activity (Fig. 7, and Fig. 8). The resulting Pareto fronts presented much starker score diversity between the Pareto-optimal solutions than the motions from the SOTO in Exp. 2 (Fig. 5). This likely happened because NSGA-II is a global optimizer, therefore, it explores the optimization space more efficiently than local optimizers. This diversity gives more options, and flexibility for the user to choose a Pareto-optimal solution according to given criteria.

To illustrate the advantage of using the MOTO approach, we visually selected some motions from each Pareto front of each activity with reasonable trade-offs between the scores (Fig. 7, Fig. 8), and compared them to the single objective solutions of the same scores (Table III). For activity A, $w^{\star}_{A3}$ had similar elbow flexion trajectory to the SOTO w.r.t. torque shoulder score, as a matter of fact, this is a good solution if the user does not care about the generalized increase in the whole-body torques (indicated by $\mathcal{J}_{nwe}$). On the other hand, if both the whole-body torques and the torques at the shoulder are important for the user, $w^{\star}_{A4}$ could be a more interesting choice. Similarly for activity B, $w^{\star}_{B2}$ is a movement that optimizes both shoulder and lumbar torques simultaneously, but if the user would prefer the minimum shoulder torques from the pareto front, then $w^{\star}_{B1}$, with less knee flexion, would be a better choice. Note that $w^{\star}_{B1}$, also has a greater reduction on the lumbar torques than the SOTO solution for the shoulder torques. Additionally, most solutions from the Pareto fronts have improved their ergonomics scores, even for scores that were not being optimized (Fig. 6). This is likely due to those scores not being in conflict with the optimized ones.

TABLE III: Improvement of the ergonomics scores w.r.t. the initial motion after SOTO and MOTO. The multi-objective solutions are indicated in the Pareto fronts (Figs. 7 and 8).

(a) Activity A

Motion	$\mathcal{J}_{tsh}$	$\mathcal{J}_{nwe}$	$\mathcal{J}_{rc}$
Initial	100%	100%	100%
Single Obj. $\mathcal{J}_{tsh}$	39.4%	146.2%	105.7%
Single Obj. $\mathcal{J}_{nwe}$	99.1%	80.2%	102.4%
Single Obj. $\mathcal{J}_{rc}$	77.6%	90.8%	95.5%
Multi-Obj. $w^{\star}_{A1}$	83.9%	115.9%	93.4%
Multi-Obj. $w^{\star}_{A2}$	72.9%	41.2%	102.7%
Multi-Obj. $w^{\star}_{A3}$	50.1%	198.0%	100.5%
Multi-Obj. $w^{\star}_{A4}$	35.8%	53.4%	97.0%

(b) Activity B

Motion	$\mathcal{J}_{tsh}$	$\mathcal{J}_{tlb}$
Initial	100%	100%
Single Obj. $\mathcal{J}_{tsh}$	33.6%	70.6%
Single Obj. $\mathcal{J}_{tlb}$	78.8%	32.8%
Multi-Obj. $w^{\star}_{B1}$	16.0%	36.9%
Multi-Obj. $w^{\star}_{B2}$	22.4%	26.0%
Multi-Obj. $w^{\star}_{B3}$	73.4%	24.4%

Video: To show that Pareto-optimal solutions obtained by MOTO are better ergonomics trade-offs than those obtained by SOTO, we refer the reader to the video attachment where we compare the different whole-body movements executed by our DHM. Clearly, optimizing for a single criteria easily produces unrealistic movements that one could actually refer to as "non ergonomic": for example, we point out the solution in activity A that minimizes only the lumbar torques with a very awkward non-ergonomic motion from other points of view. Movements generated by our MOTO approach are more feasible and ergonomically reasonable.

In conclusion, generating whole-body motion with MOTO provides better trade-offs among several ergonomics criteria; and because many solutions are generated, we obtain a tool that enables a user (i.e., an ergonomist) to choose from a set of ergonomic motions that are often better than the ones generated with SOTO.

VI. Conclusions

We proposed a simulation-based MOTO framework to generate user- and task-specific ergonomic whole-body motions that simultaneously optimize several ergonomics criteria.

We showed that single-objective optimization may not be sufficient to obtain "good" ergonomic motions, since optimizing for only one criterion often produces motions that are less ergonomic in other body regions. In our approach, instead, we generate a set of Pareto-optimal motions that trade-offs ergonomics scores. Our framework can be used to select trajectories from the Pareto front, to recommend better motions to workers, or even input them as a reference to a human-robot interaction controller to assist or influence the human motion behavior. In the future, we plan to collaborate with

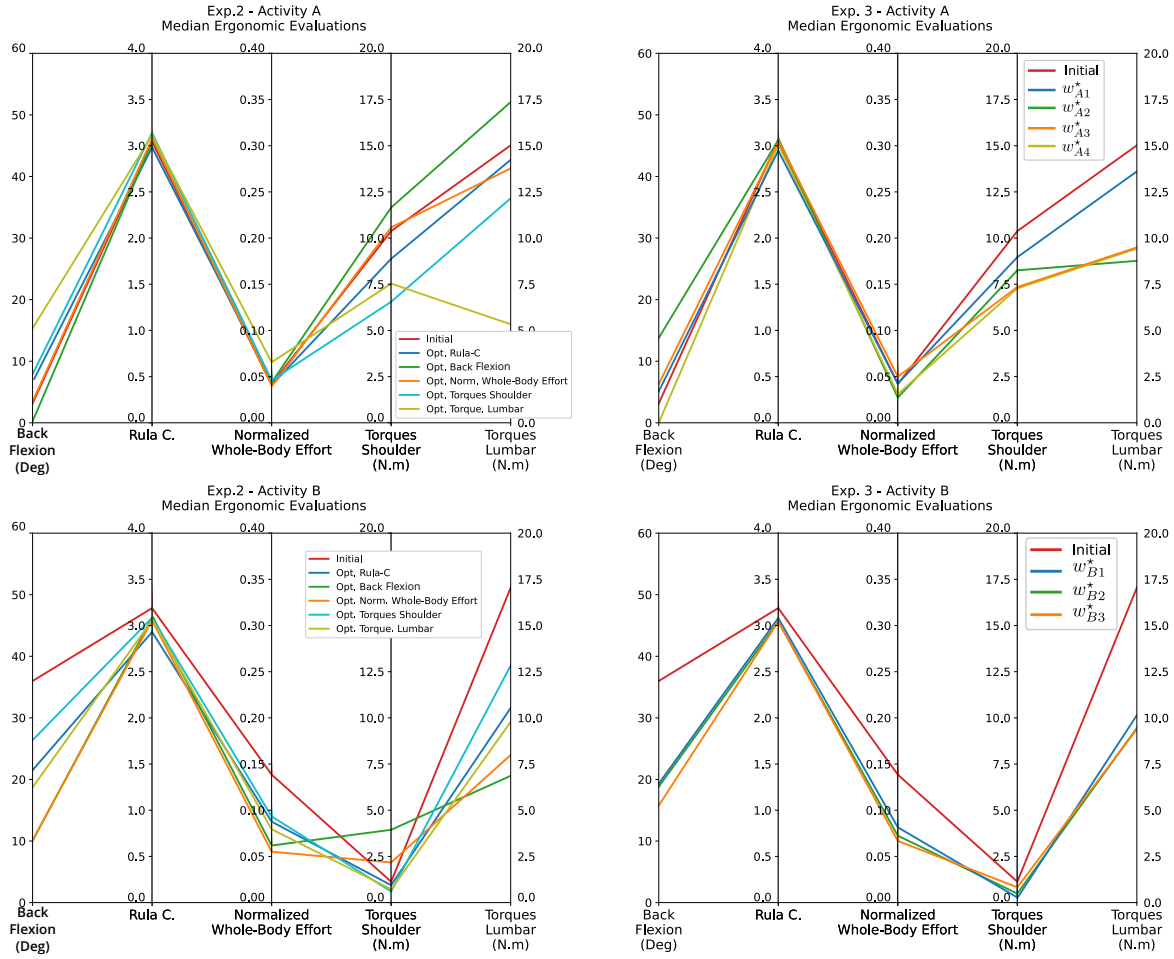

Fig. 5: Experiment 2 (SOTO) and Experiment 3 (MOTO) - The median of the ergonomics scores during the execution of the initial and optimal motions. Lines of the same color represent one motion, and each axis represents one of the ergonomics scores. The motions in experiment 2 are taken from 5 independent single-objective optimizations for each activity. The motions in experiment 3 are taken from the respective Pareto fronts for each activity (Fig. 7 and 8).

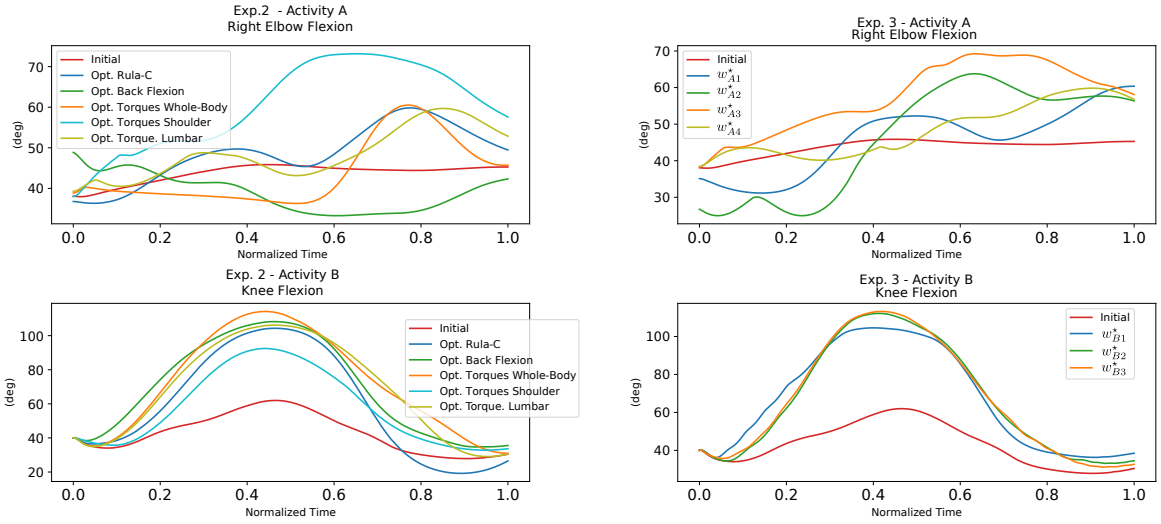

Fig. 6: Experiment 2 (SOTO) and Experiment 3 (MOTO) - Time evolution of selected angles of the initial movement and the optimized motions: elbow flexion for activity A (Reaching); knee flexion for activity B (Lifting).

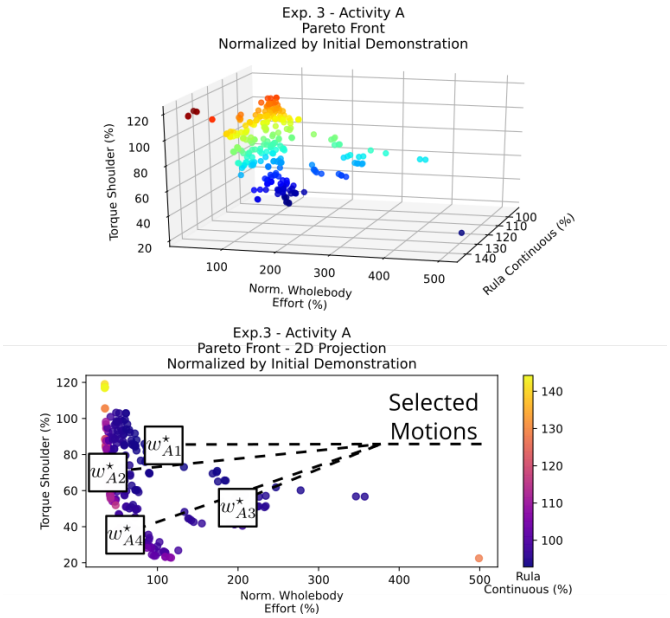

Fig. 7: Experiment 3 - Activity A - Pareto front. The ergonomics scores values are normalized by those of the initial motion. The bottom image is a 2D projection of the 3D Pareto front, the third objective is represented by a color scale on each point.

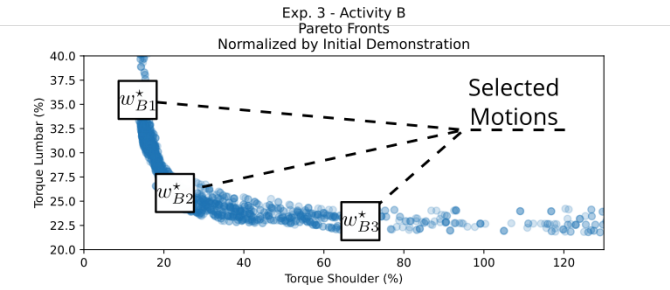

Fig. 8: Experiment 3 - Activity B - Pareto front. The ergonomics scores values are normalized by those of the initial motion.

ergonomics experts to validate the use of our tool for occupational ergonomics and ergonomic human-robot collaboration.

References

[1] L. Punnett and D. H. Wegman, "Work-related musculoskeletal disorders: the epidemiologic evidence and the debate," *Journal of electromyography and kinesiology*, vol. 14, no. 1, pp. 13–23, 2004.

[2] K. K. Lett and S. M. McGill, "Pushing and pulling: personal mechanics influence spine loads," *Ergonomics*, vol. 49, no. 9, pp. 895–908, 2006.

[3] B. Busch, G. Maeda, Y. Mollard, M. Demangeat, and M. Lopes, "Postural optimization for an ergonomic human-robot interaction," in *2017 IEEE/RSJ International Conference on Intelligent Robots and Systems (IROS)*. IEEE, 2017, pp. 2778–2785.

[4] W. Kim, J. Lee, L. Peternel, N. Tsagarakis, and A. Ajoudani, "Anticipatory robot assistance for the prevention of human static joint overloading in human–robot collaboration," *IEEE robotics and automation letters*, 2018.

[5] A. G. Marin, M. S. Shourijeh, P. E. Galibarov, M. Damsgaard, L. Fritzsch, and F. Stulp, "Optimizing contextual ergonomics models in human-robot interaction," in *2018 IEEE/RSJ International Conference on Intelligent Robots and Systems (IROS)*. IEEE, 2018, pp. 1–9.

[6] A. Shafti, A. Ataka, B. U. Lazpita, A. Shiva, H. A. Wurdemann, and K. Althoefer, "Real-time robot-assisted ergonomics," in *2019 International Conference on Robotics and Automation (ICRA)*. IEEE, 2019.

[7] B. Busch, M. Toussaint, and M. Lopes, "Planning ergonomic sequences of actions in human-robot interaction," in *2018 IEEE International Conference on Robotics and Automation (ICRA)*, 2018, pp. 1916–1923.

[8] P. Maurice, V. Padois, Y. Measson, and P. Bidaud, "Assessing and improving human movements using sensitivity analysis and digital human simulation," *International Journal of Computer Integrated Manufacturing*, pp. 1–13, 2019.

[9] S. Scataglini and G. Paul, *DHM and Posturography*. Elsevier Science, 2019.

[10] L. v. der Spaa, M. Gienger, T. Bates, and J. Kober, "Predicting and optimizing ergonomics in physical human-robot cooperation tasks," in *2020 IEEE International Conference on Robotics and Automation (ICRA)*, 2020, pp. 1799–1805.

[11] R. Rahal, G. Matarese, M. Gabiccini, A. Artoni, D. Prattichizzo, P. R. Giordano, and C. Pacchierotti, "Caring about the human operator: Haptic shared control for enhanced user comfort in robotic telemanipulation," *IEEE Transactions on Haptics*, vol. 13, no. 1, pp. 197–203, 2020.

[12] A. Yazdani and R. S. Novin, "Posture estimation and optimization in ergonomically intelligent teleoperation systems," *International Conference on Human-Robot Interaction*, 2021.

[13] Y. Xiang, J. S. Arora, S. Rahmatalla, T. Marler, R. Bhatt, and K. Abdel-Malek, "Human lifting simulation using a multi-objective optimization approach," *Multibody System Dynamics*, 2010.

[14] A. Iriondo Pascual, D. Högberg, A. Syberfeldt, F. García Rivera, E. Pérez Luque, and L. Hanson, "Implementation of ergonomics evaluation methods in a multi-objective optimization framework," in *6th International Digital Human Modeling Symposium, August 31-September 2, 2020, Skövde, Sweden*. IOS Press, 2020, pp. 361–371.

[15] P. Maurice, V. Padois, Y. Measson, and P. Bidaud, "Human-oriented design of collaborative robots," *International Journal of Industrial Ergonomics*, vol. 57, pp. 88–102, 2017.

[16] L. F. C. Figueredo, R. C. Aguiar, L. Chen, S. Chakrabarty, M. R. Dogar, and A. G. Cohn, "Human comfortability: Integrating ergonomics and muscular-informed metrics for manipulability analysis during human-robot collaboration," *IEEE Robotics and Automation Letters*, 2021.

[17] D. Chaffin, G. Andersson, and B. Martin, *Occupational Biomechanics*. Wiley, 2006.

[18] Open Design Lab, Penn State University, "Open design lab scaling calculator," http://tools.openlab.psu.edu/tools/proportionality_constants.htm, accessed: 2020-01-10.

[19] J. Lee, M. X. Grey, S. Ha, T. Kunz, S. Jain, Y. Ye, S. S. Srinivasa, M. Stilman, and C. K. Liu, "DART: Dynamic animation and robotics toolkit," *Journal of Open Source Software*, 2018.

[20] E. Mingo Hoffman, A. Rocchi, A. Laurenzi, and N. G. Tsagarakis, "Robot control for dummies: Insights and examples using opensot," in *2017 IEEE-RAS 17th International Conference on Humanoid Robotics (Humanoids)*, Nov 2017, pp. 736–741.

[21] G. David, "Ergonomic methods for assessing exposure to risk factors for work-related musculoskeletal disorders," *Occupational medicine*, vol. 55, no. 3, pp. 190–199, 2005.

[22] L. McAtamney and N. Corlett, "Rula: a survey method for the investigation of work-related upper limb disorders," *Applied Ergonomics*, 1993.

[23] A. Paraschos, C. Daniel, J. Peters, and G. Neumann, "Using probabilistic movement primitives in robotics," *Autonomous Robots*, 2018.

[24] W. Gomes, V. Radhakrishnan, L. Penco, V. Modugno, J. Mouret, and S. Ivaldi, "Humanoid whole-body movement optimization from retargeted human motions," in *2019 IEEE-RAS 19th International Conference on Humanoid Robots (Humanoids)*, 2019, pp. 178–185.

[25] M. J. Powell, "A direct search optimization method that models the objective and constraint functions by linear interpolation," in *Advances in optimization and numerical analysis*. Springer, 1994, pp. 51–67.

[26] S. G. Johnson, *The NLopt nonlinear-optimization package*. [Online]. Available: http://ab-initio.mit.edu/nlopt

[27] K. Deb, "Multi-objective optimisation using evolutionary algorithms: an introduction," in *Multi-objective evolutionary optimisation for product design and manufacturing*. Springer, 2011, pp. 3–34.

[28] J.-B. Mouret and S. Doncieux, "SFERESv2: Evolvin' in the multi-core world," in *Proc. of Congress on Evolutionary Computation (CEC)*, 2010.